Supplementary information

for

Aggregation-induced delayed fluorescence luminogens: the innovation of purely organic emitters for aqueous electrochemiluminescence

Baohua Zhang,[a] Yi Kong,[a] Huijun Liu,[b] Bin Chen,[b] Bolin Zhao,[a] Yelin Luo,[a] Lijuan Chen,[a] Yuwei Zhang,[a] Dongxue Han,[a] Zujin Zhao,*[b] Ben Zhong Tang*[b,c] and Li Niu*[a]

[a] Centre for Advanced Analytical Science, c/o School of Chemistry and Chemical Engineering, Guangzhou Key Laboratory of Sensing Materials & Devices, Guangzhou University, Guangzhou 510006, P. R. China. E-mail: lniu@gzhu.edu.cn

[b] State Key Laboratory of Luminescent Materials and Devices, Guangdong Provincial Key Laboratory of Luminescence from Molecular Aggregates, South China University of Technology, Guangzhou 510640, China. E-mail: mszjzhao@scut.edu.cn; tangbenz@ust.hk

[c] Shenzhen Institute of Aggregate Science and Technology, School of Science and Engineering, The Chinese University of Hong Kong, Shenzhen, Guangdong 518172, China.

*Corresponding authors.

E-mail address: lniu@gzhu.edu.cn (L. Niu); mszjzhao@scut.edu.cn (Z.-J. Zhao); tangbenz@ust.hk (B.-Z. Tang)

Supplementary Figures and Tables

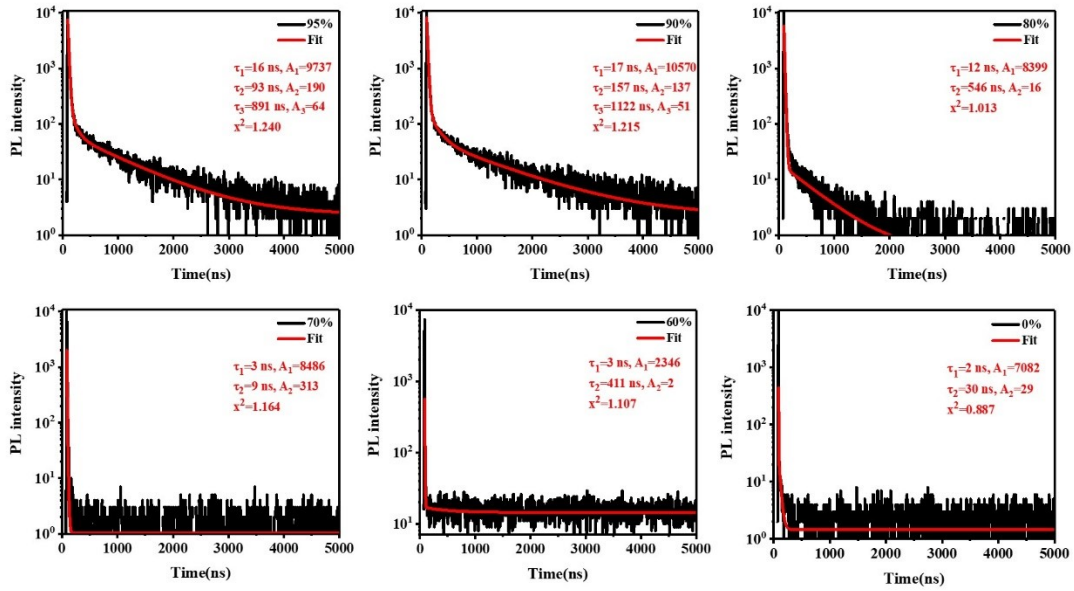

Figure S1. The transient PL decay curves and their exponential fitting results of the AIDF molecule, i.e. mCP-BP-PXZ, in THF/water mixtures with different water fractions (f_w), i.e. 0 %, 60 %, 70 %, 80 %, 90 %, 95 % (excitation wavelength: 363 nm, and detection wavelength: 553 nm) at 300 K.

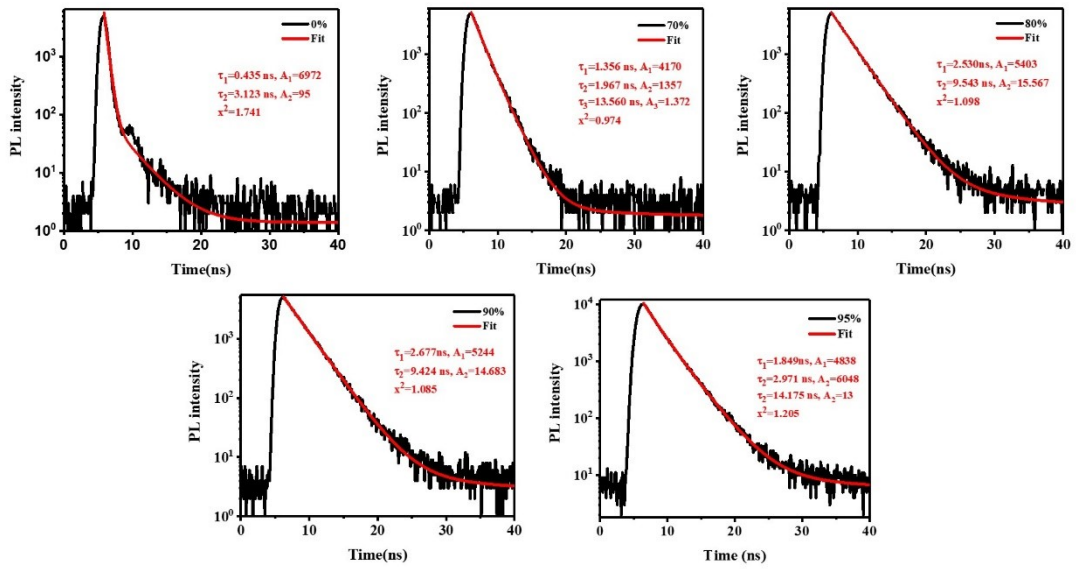

Figure S2. The transient PL decay curves and their exponential fitting results of the AIE molecule, i.e. TPE-TAPBI, in THF/water mixtures with different water fractions (f_w), i.e. 0 %, 70 %, 80 %, 90 %, 95 % (excitation wavelength: 363 nm, and detection wavelength: 454 nm) at 300 K.

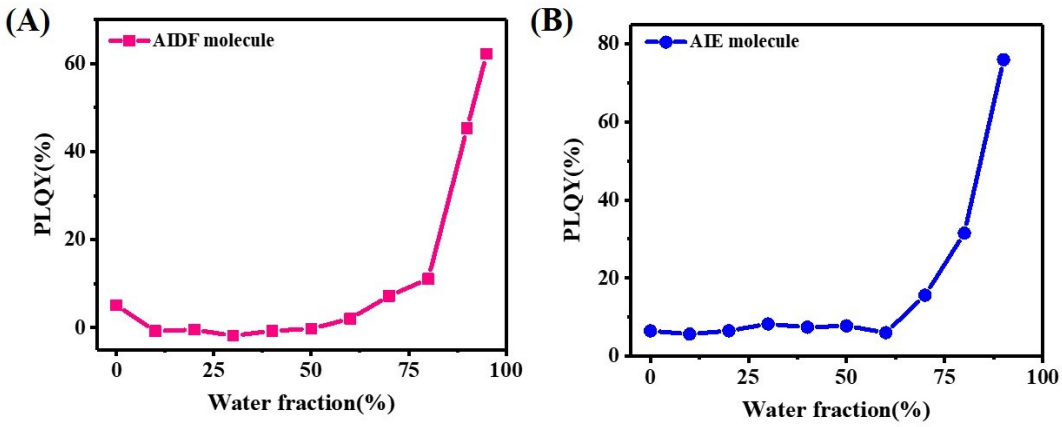

Figure S3. PL quantum efficiency (PLQY) of the (A) AIDF molecule, i.e. mCP-BP-PXZ and (B) AIE molecule, i.e. TPE-TAPBI, in THF/water mixtures with different water fractions (f_w).

Table S1. The photophysical properties of the AIDF molecule, i.e. mCP-BP-PXZ, in THF/water mixtures with different water fractions (f_w).

Molecule (f_w)	λ_{em} [a] [nm]	Φ_{PL} [b] [%]	τ_p/τ_d [c] [ns]/[ns]	Φ_{PF}/Φ_{DF} [d] [%]/[%]	k_f [e] [10^7 s^{-1}]	k_{ISC} [f] [10^7 s^{-1}]	k_{RISC} [g] [10^6 s^{-1}]
mCP-BP-PXZ (95 %)	553	62.2	16/702	42.1/20.1	2.63	3.62	1.17
mCP-BP-PXZ (90 %)	553	45.3	17/858	31.5/13.8	1.85	4.03	0.76
mCP-BP-PXZ (80 %)	555	11.1	12/546	10.2/0.9	0.85	7.48	0.18

mCP-BP-PXZ (0 %)	618	5.1	3.6/-	5.1/-	1.42	26.4[h]	-

[a] Measured in THF/water mixtures at room temperature. [b] Absolute PLQY evaluated using an integrating sphere under air atmosphere. [c] The prompt fluorescence lifetime (τ_p) and the delayed fluorescence lifetime (τ_d) calculated by PL decay curves from 0 to 5 μs under air atmosphere at 300 K, the average lifetime calculated by $\tau_{av} = \sum A_i\tau_i^2/\sum A_i\tau_i$, where A_i is the pre-exponential for lifetime τ_i (A_i and τ_i are shown in Figure S1). [d] The fractional contributions of the prompt fluorescence (Φ_{PF}) and delayed fluorescence (Φ_{DF}) to the total Φ_{PL} calculated by emission decay curves from 0 to 5 μs under air atmosphere. $\Phi_{PL} = \Phi_{PF} + \Phi_{DF}$, $\Phi_{PF} = r_{prompt} \times \Phi_{PL}$, $r_{prompt} = \tau_1A_1/(\tau_1A_1 + \tau_2A_2 + \tau_3A_3)$, $\Phi_{DF} = r_{delayed} \times \Phi_{PL}$, $r_{delayed} = 1 - r_{prompt}$. [e] The fluorescence rate constants of S_1 calculated using equation of $k_f = \Phi_{PF}/\tau_p$. [f] The rate constants of ISC calculated using equation of $k_{ISC} = 1/\tau_p(1-\Phi_{PF})$. [g] The rate constant of RISC rate was calculated using equation of $k_{RISC} = (k_pk_d)/k_{ISC} \times (\Phi_{DF}/\Phi_{PF})$, in which $k_p = 1/\tau_p$, $k_d = 1/\tau_d$. [h] Herein, this rate stands for nonradiative decay rate for this sample without distinct delayed fluorescent property, i.e. $k_{nr} = k_p - k_f$.

Table S2. The photophysical properties of the AIE molecule, i.e. TPE-TAPBI, in THF/water mixtures with different water fractions (f_w).

Molecule (f_w)	λ_{em}[a] [nm]	Φ_{PL}[b] [%]	τ_p[c] [ns]	k_f[d] [10^8 s^{-1}]	k_{nr}[e] [10^8 s^{-1}]
TPE-TAPBI (90 %)	454	75.9	2.7	2.8	0.9
TPE-TAPBI (80 %)	452	31.5	2.5	1.3	2.7
TPE-TAPBI (70 %)	449	15.6	1.6	1.0	5.3

TPE-TAPBI (0 %)	448	6.5	0.7	0.9	13.4

[a] Measured in THF/water mixtures at room temperature. [b] Absolute PL quantum yield evaluated using an integrating sphere under air atmosphere. [c] The prompt fluorescence lifetime (τ_p) calculated by emission decay curves from 0 to 40 ns under air atmosphere at 300 K, the average lifetime calculated by $\tau_{av} = \sum A_i\tau_i^2/\sum A_i\tau_i$, where A_i is the pre-exponential for lifetime τ_i (A_i and τ_i are shown in Figure S2). [d] The radiative fluorescent decay rate from S_1 to S_0 level, $k_f = \Phi_{PL}/\tau_p$. [e] The nonradiative decay rate from S_1 to S_0 level, $k_{nr} = 1/\tau_p - k_f$.

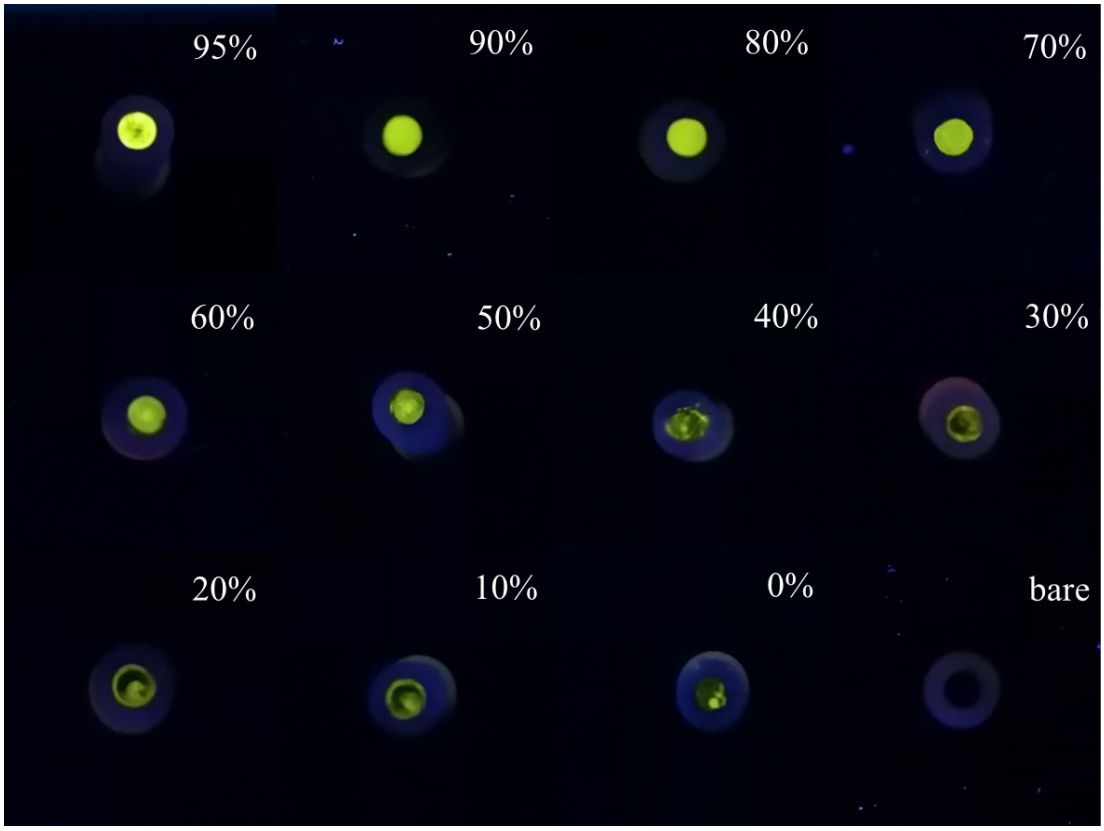

Figure S4. The UV irradiation (λ = 365 nm) photographs of GCE modified with AIDF molecule, i.e. mCP-BP-PXZ (pre-aggregated solution condition: mCP-BP-PXZ luminogen solution dissolved in THF/H_2O mixtures with different water fractions).

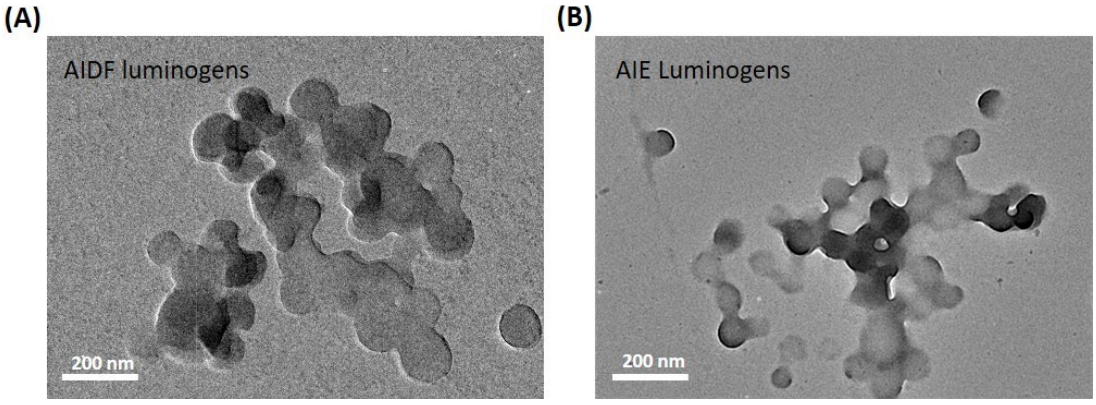

Figure S5. TEM characterizations of dip-coated film morphology of AIDF luminogen solution (A), i.e. mCP-BP-PXZ, or AIE luminogen solution (B), i.e. TPE-TAPBI, (pre-aggregated solution condition: 0.1 mM, f_w = 95 %).

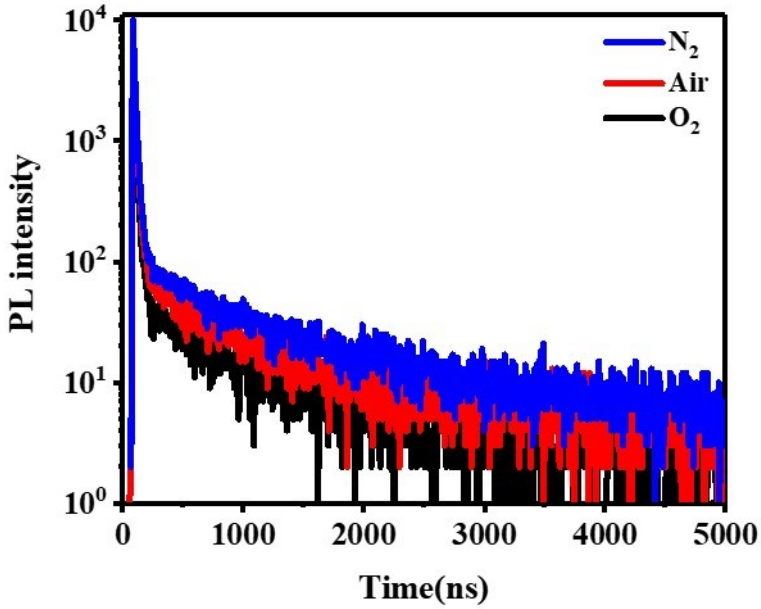

Figure S6. The transient PL decay curves of the AIDF molecule, i.e. mCP-BP-PXZ (f_w = 95 %) dip-coated film under different atmosphere condition, i.e. nitrogen, air, oxygen (excitation wavelength: 363 nm, and detection wavelength: 542 nm) at 300 K.

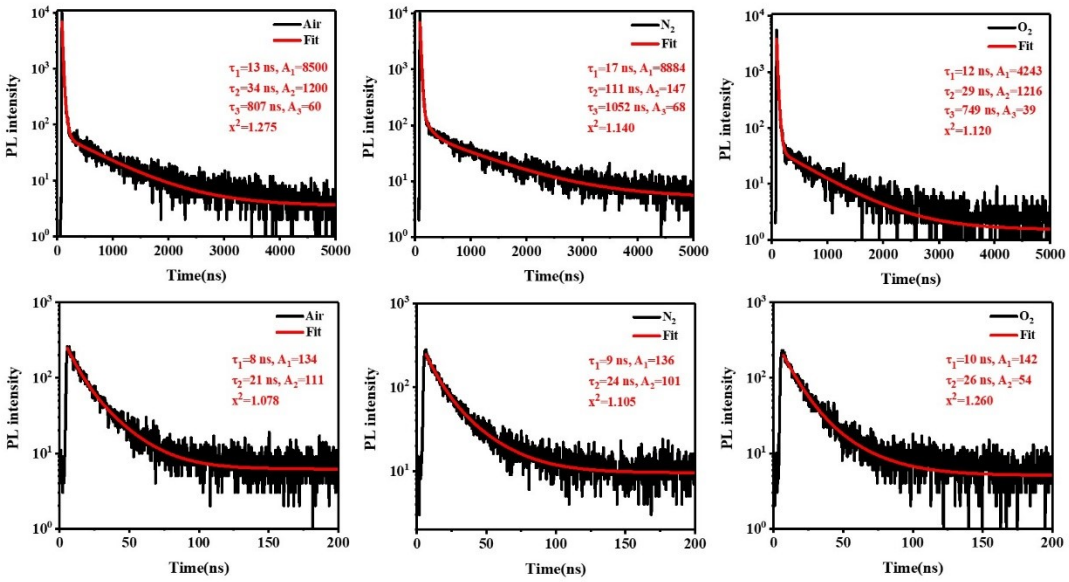

Figure S7. The transient PL decay curves and their exponential fitting results of the AIDF molecule, i.e. mCP-BP-PXZ (f_w = 95%) dip-coated film under different atmosphere condition, i.e. nitrogen, air, oxygen (excitation wavelength: 363 nm, and detection wavelength: 542 nm) at 300 K.

Table S3. The photophysical properties of the AIDF molecule, mCP-BP-PXZ (f_w = 95 %) dip-coated film under different atmosphere condition.

film	λ_{abs} [a] [nm]	λ_{em} [a] [nm]	Φ_{PL} [b] [%]	τ_p/τ_d [c] [ns]/[ns]			Φ_{PF}/Φ_{DF} [d] [%]/[%]	k_f [e] [10^7 s^{-1}]	k_{ISC} [f] [10^7 s^{-1}]	k_{RISC} [g] [10^6 s^{-1}]
				air	N_2	O_2				
mCP-BP-PXZ	344,330, 297	542	28.3	17/ 453	19/ 877	18/ 355	15.6/12.7	0.9	5.0	2.1

[a] Measured in neat film at room temperature. [b] Absolute PL quantum yield evaluated using an integrating sphere under air atmosphere. [c] The prompt fluorescence lifetime (τ_p) and the delayed fluorescence lifetime (τ_d) calculated by emission decay curves from 0 to 5 μs under air, nitrogen and oxygen atmosphere at 300 K. [d] The fractional contributions of the fluorescence (Φ_F) and TADF (Φ_{TADF}) to the total Φ_{PL} calculated by emission decay curves from 0 to 5 μs under air atmosphere. $\Phi_{PL} = \Phi_{PF} + \Phi_{DF}$, $\Phi_{PF} = r_{prompt} \times \Phi_{PL}$, $r_{prompt} = \tau_1 A_1/(\tau_1 A_1 + \tau_2 A_2 + \tau_3 A_3)$, $\Phi_{DF} = r_{delayed} \times \Phi_{PL}$, $r_{delayed} = 1 - r_{prompt}$. [e] The fluorescence rate constants of S_1 calculated using equation of $k_f = \Phi_{PF}/\tau_p$. [f] The rate constants of ISC calculated using equation of $k_{ISC} = 1/\tau_p(1-\Phi_{PF})$. [g] The rate constant of RISC rate was calculated using equation of $K_{RISC} = (k_p k_d)/K_{ISC} \times (\Phi_{DF}/\Phi_{PF})$, in which $k_p = 1/\tau_p$, $k_d = 1/\tau_d$.

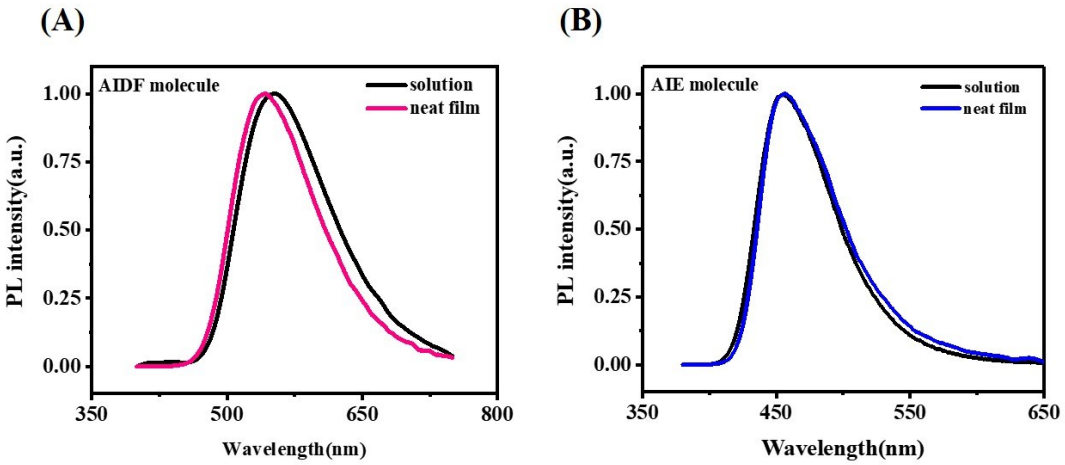

Figure S8. Normalized PL spectra of the AIDF luminogen, i.e. mCP-BP-PXZ, or AIE luminogen, i.e. TPE-TAPBI (f_w = 95 %) in PBS solution or in dip-coated neat film.

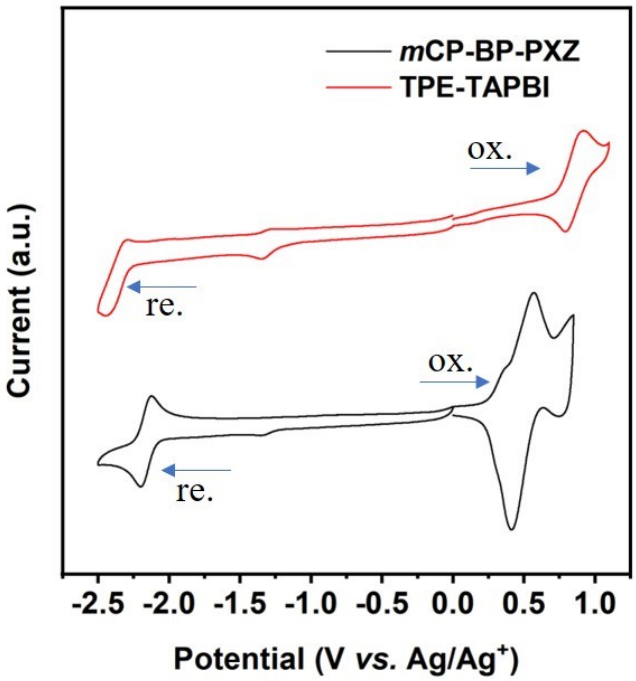

Figure S9. Cyclic voltammograms of mCP-BP-PXZ and TPE-TAPBI in solution (1 mM) (measured in high purity nitrogen-filled glovebox, using the solvent of dichloromethane (DCM) and acetonitrile (ACN) for oxidation and reduction scan, respectively. 0.1 M $TBAPF_6$, scan rate: 0.1 V s^{-1}, potential versus Ag/Ag^+).

Table S4. Electrochemical data of AIDF molecule, i.e. mCP-BP-PXZ, and AIE molecule, i.e. TPE-TAPBI, and the calculated energy levels and energy gap.

Molecule	$E_{1/2}^{OX}$ [a)] [V]	$E_{1/2}^{Red}$ [a)] [V]	HOMO [b)] [eV]	LUMO [b)] [eV]	E_g [b)] [eV]
mCP-BP-PXZ	0.49	-2.16	-5.09	-2.60	2.49
TPE-TAPBI	0.85	- [c)]	-5.46	-2.67 [d)]	2.93 [e)]

[a)] Potential was versus Ag/Ag^+, in which $E_{1/2}^{OX}$ and $E_{1/2}^{Red}$ are the half wave potential for oxidation and reduction, respectively (calculated as the mean value of the redox peaks) [s1, s2]. [b)] Ferrocene couple (Fc/Fc^+) was used as the internal reference. The energy levels were calculated using the following equations: $E_{HOMO} = -(E_{1/2}^{Ox} - E_{Fc/Fc^+} + 4.8)$ eV, $E_{LUMO} = -(E_{1/2}^{Red} - E_{Fc/Fc^+} + 4.8)$ eV, $E_g = E_{LUMO} - E_{HOMO}$. [c)] not precisely available due to irreversible redox process. [d)] $E_{LUMO} = E_g + E_{HOMO}$. [e)] from ref. [s3], i.e. optical bandgap calculated from the onset of the absorption spectrum.

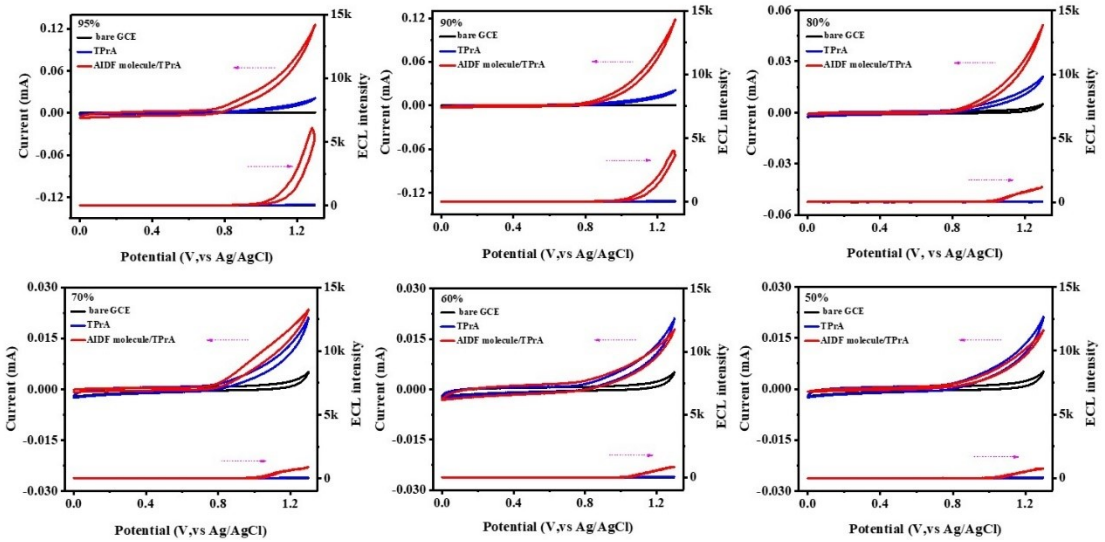

Figure S10. Anodic cyclic voltammograms and the corresponding oxidative-reduction ECL responses of bare GCE, or bare GCE/40 mM TPrA or AIDF-luminogen-modified GCE/40 mM TPrA couple (while the dip-coated AIDF film was fabricated by using different AIDF luminogen solution in THF/water mixtures with different water fractions, i.e. 50 % - 95 %. CV/ECL test conditions: a potential window ranging from 0 V to 1.3 V (vs, Ag/AgCl), scan rate: 0.5 V s^{-1}, 0.1 M PBS containing 0.1 M KCl, pH: 7.44. PMT Voltage: 850 V.

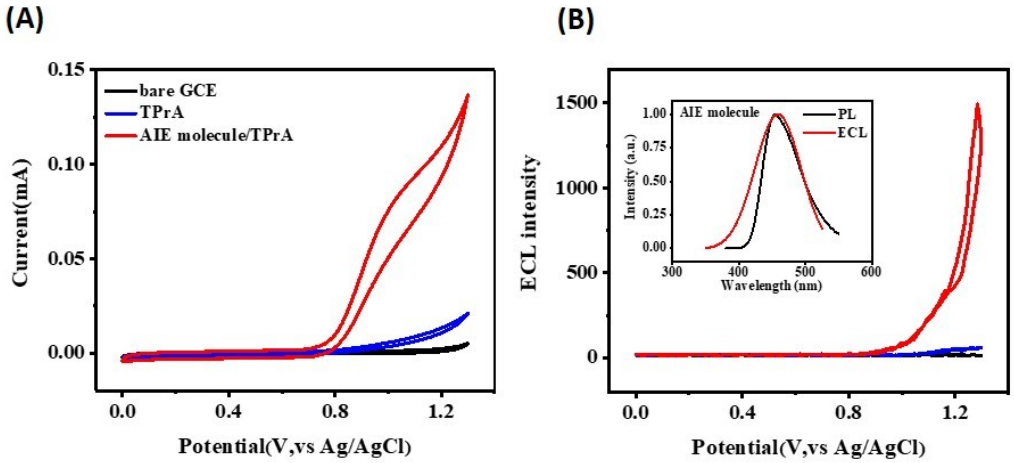

Figure S11. (A) Anodic cyclic voltammograms and (B) the corresponding oxidative-reduction ECL responses of bare GCE, or bare GCE/40 mM TPrA or AIE-luminogen-modified GCE/40 mM TPrA couple (Condition: the dip-coated AIE-luminogen-modified GCE used the TPE-TAPBI luminogen solution in THF/water mixture containing the water fraction of 95%). Inset: PL and ECL spectra of the AIE molecule in the solid state. CV/ECL test condition: a potential window ranging from 0 V to 1.3 V (vs, Ag/AgCl), scan rate: 0.5 V s^{-1}, 0.1 M PBS containing 0.1 M KCl, pH: 7.44. PMT: 850 V.

Table S5. The details about the integrated current and ECL intensity signals for

calculating the relative ECL efficiency of TPE-TAPBI (f_w: 95 %)-luminogen-modified GCE/TPrA vs. mCP-BP-PXZ (f_w: 95 %)-luminogen-modified GCE/TPrA in the PBS medium.

System	$\int_a^b Idt$	$\int_a^b idt$	Φ_{ECL} [%]
TPE-TAPBI/TPrA	536.26	1.39	100
mCP-BP-PXZ/TPrA	2217.52	1.06	540

Table S6. Main photophysical and ECL parameters for the AIDF molecule, i.e. mCP-BP-PXZ, and the AIE molecule, i.e. TPE-TAPBI, respectively.

Molecule	f_w (vol%)	PL lifetime [a]		λ_{PL} [nm]	λ_{ECL} [c] [nm]	Φ_{PL} [d] [%]	Φ_{ECL} [e] [%]
		τ_{PF} (ns)	τ_{DF} (ns)				
mCP-BP-PXZ	95	17	453	542 [a] 553 [b]	596	28.3	540
TPE-TAPBI	95	2.7	-	456 [a] 454 [b]	477	34.0	100

[a] Tested for neat dip-coated film (f_w: 95 %) in air. [b] Tested for the solution (f_w: 95 %). [c] ECL peak position for oxidative-reduction ECL with TPrA. [d] Absolute PLQY evaluated using an integrating sphere under air atmosphere. [e] Relative ECL efficiency of mCP-BP-PXZ -modified GCE (f_w: 95 %)/TPrA (40 mM) vs. TPE-TAPBI -modified GCE (f_w: 95 %)/TPrA (40 mM) reference (setting as 100 %).

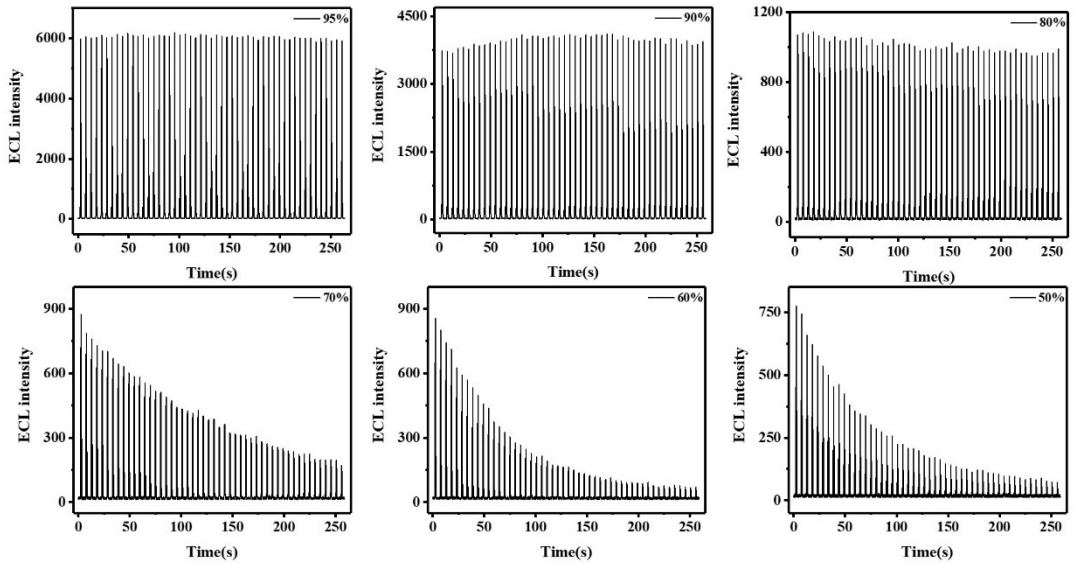

Figure S12. ECL stability test (50 cycles) for the AIDF-luminogen-modified GCE/TPrA couple (the dip-coated mCP-BP-PXZ solution contained different water fractions ranging from 50 % to 95 %. ECL test condition: a potential window: 0 V-1.3 V (vs, Ag/AgCl), scan rate: 0.5 V s^{-1}, 0.1 M PBS containing 0.1 M KCl and 40 mM TPrA, pH: 7.44. PMT: 850 V.

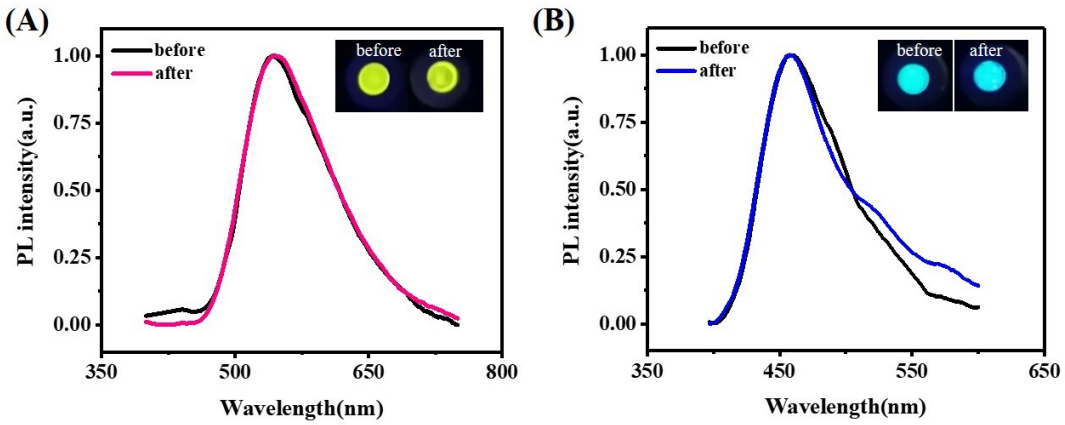

Figure S13. Normalized PL spectra of AIDF (A) or AIE (B) luminogen modified GCE sample, i.e. before and after oxidative-reduction ECL test using such sample discussed above.

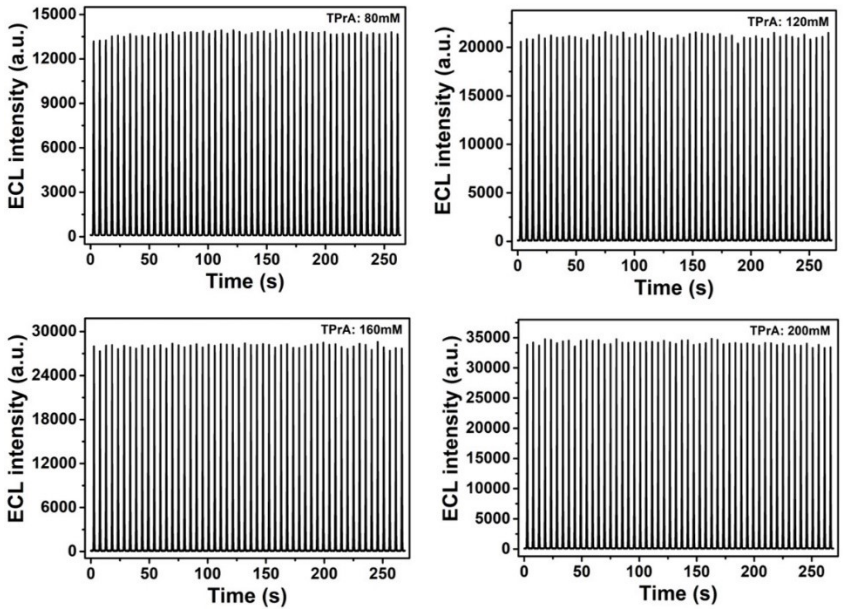

Figure S14. ECL stability test (50 cycles) for the AIDF-luminogen-modified GCE/TPrA couple (the dip-coated mCP-BP-PXZ solution contained 95% water fraction. ECL test condition: a potential window: 0 V - 1.3 V (vs, Ag/AgCl), scan rate: 0.5 V s^{-1}, 0.1 M PBS containing 0.1 M KCl) using different concentration of TPrA, i.e. 80, 120, 160 and 200 mM, respectively.

Reference:

S1. H. D. Li, J. Daniel, J. B. Verlhac, M. Blanchard-Desce and N. Sojic, *Chem.-Eur. J.*, 2016, **22**, 12702-12714.
S2. K. Redin, A. D. Wilson, R. Newell, M. R. DuBois and D. L. DuBois, *Inorg. Chem.*, 2007, **46**, 1268-1276.
S3. B. Chen, B. Q. Liu, J. J. Zeng, H. Nie, Y. Xiong, J. H. Zou, H. L. Ning, Z. M. Wang, Z. J. Zhao and B. Z. Tang, *Adv. Funct. Mater.*, 2018, **28**, 1803369.